Spintronics

S.D. Bader[1] and S.S.P. Parkin[2]

[1]Materials Science Division and Center for Nanoscale Materials, Argonne National Laboratory, Argonne, Illinois 60439; email: bader@anl.gov

[2]IBM Almaden Research Center, San Jose, California 95120

Annu. Rev. Condens. Matter Phys. 2010. 1:71–88

First published online as a Review in Advance on April 9, 2010

The *Annual Review of Condensed Matter Physics* is online at conmatphys.annualreviews.org

This article's doi:
10.1146/annurev-conmatphys-070909-104123

1947-5454/10/0810-0071$20.00

Abstract

Spintronics encompasses the ever-evolving field of magnetic electronics. It is an applied discipline that is so forward-looking that much of the research that supports it is at the center of basic condensed matter physics. This review provides a perspective on recent developments in switching magnetic moments by spin-polarized currents, electric fields, and photonic fields. Developments in the field continue to be strongly dependent on the exploration and discovery of novel material systems. An array of novel transport and thermoelectric effects dependent on the interplay between spin and charge currents have been explored theoretically and experimentally in recent years. The review highlights select areas that hold promise for future investigation and attempts to unify and further inform the field.

1. INTRODUCTION

Spintronics is blossoming with new physics and potential for practical consequences in the marketplace. Spintronics is one of the emerging disciplines that continues to revolutionize the thriving field of information technology. Information technology has been a wellspring of intellectual and economic vitality in the modern world. This review provides a glimpse of the diverse ways that spin-polarized electrons can reveal themselves, such as in confined systems, in physical proximity in novel geometries, and on ultrashort time scales. The review is concerned mostly with nanomagnetic systems, including ordinary ferromagnets. However, when confined, or on ultrafast time scales or in nonequilibrium configurations, exotic behavior can ensue that has never before been dreamt of in the more than four hundred year history of the science of magnetism. For a brief history of the scientific discipline of magnetism from the time of William Gilbert's publication of *De Magnete* in 1600, regarded as the first text to embrace the scientific method of inquiry, to our modern era of nanomagnetism, with its swirling magnetic vortex structures on length scales and timescales unimaginable in Shakespearean times, see Reference 1.

The commercial impact of spintronics to date has been in the area of spin valves used in magnetic hard disk drives. The principle of operation of such spin valves is based on the giant magnetoresistive (GMR) effect, for which the Nobel Prize in Physics was awarded in 2007 to Albert Fert and Peter Grünberg. In the GMR effect, two ferromagnetic layers sandwich a nonferromagnetic metal spacer of nanometer thickness. When the magnetizations of the two ferromagnetic layers are parallel, the valve is open or in a low resistance state. When the two are antiparallel, the valve is closed or in a high resistance state. The spin valve acts as a sensor as it flies above the magnetic recording medium, sensing transitions between bits as their stray field reverses. Although GMR spin valves and advanced magnetic media led to strikingly dramatic increases in areal storage density of hard disk drives, technologies continue to supersede one another and the GMR era is already passé, having lasted all of ten years. It has now been replaced by recently developed spin-dependent tunneling devices, in which the metal spacer is replaced by an insulating barrier, and the magnetoresistance of the device increases at room temperature relative to the GMR counterpart by a factor of ten in applications involving sensing for disk drives. These sensing heads are known as magnetic tunnel junctions (MTJs) or tunneling magnetoresistance (TMR) devices. MTJ devices were introduced by Moodera et al. (2) and Miyazaki & Tezuka (3) who utilized amorphous barrier materials. Butler et al. (4) and Mathon & Umerski (5) calculated that crystalline MgO(001) would have superior properties, which has led to recent room-temperature TMR values as high as 600% (6) and 1000% (7). Thus, spintronics encompasses the ever-evolving field of magnetic electronics. It is an applied discipline that is so forward-looking that much of the research that supports it is at the center of basic condensed matter physics.

Although spintronic devices and prototypes are ultrasmall, in addition to the nanoscale spatial realm is the world of ultrafast phenomena. The ultrafast realm is emerging as a new scientific area as imaging experiments are conducted on a scale that uses picoseconds and femtoseconds. This review does not attempt to cover the experimental measurement and characterization methods and techniques of the spintronics field. Instead, we provide general references (8, 9) for the reader and a popular reference with respect to spintronic materials and phenomena (10), as well as some specific ones relative to magnetic microscopy (11), neutron (12), and hard (13) and soft (14) X-ray synchrotron approaches.

We also highlight a newer technique with real-time imaging because it has not been reviewed extensively. Scanning transmission X-ray microscopy (STXM), a soft X-ray scattering method, is based on circularly polarized incident X-rays and magnetic circular dichroism detection. In the referenced example (15), which is discussed in Section 2.1, the spatial resolution is 30 nm, the temporal resolution is ~100 ps, the flash repetition rate is 500 MHz, and the scan size is $2 \times 2\ \mu m^2$. These conditions are sufficient to track the magnetization dynamics of vortices in permalloy (NiFe alloy) nanostructures as they gyrate in response to high frequency, spin-polarized electric currents passing through them.

The recent ability to fabricate and pattern ultrathin (1–10 atomic layer) structures via lithographic techniques, for example, to make MTJs, has brought new science and technology to fruition. MTJ structures have been around for 30 years but have not been understood well enough to be harnessed commercially. It was thought that the spin polarization of the tunneling current was determined by the spin-polarized density of states of the electrode, and that the polarization was determined by the magnetic moment; however, the tunneling matrix elements are determined by the combined symmetry of the wavefunction of the metal and the insulator.

Electron beam lithography provides precise positioning of structures, but industrial fab lines are becoming expensive enough that innovation might get stifled. Self-assembly, a driver of the nanotechnology era, relies on inexpensive chemical processes but can lack the precise positioning of lithography because the processes are stochastic. Hybrid approaches that blend the best of lithography and self-assembly using inexpensive (imprint) lithography to guide the self-assembly appear quite attractive (1). Bio-inspired self-assembly that

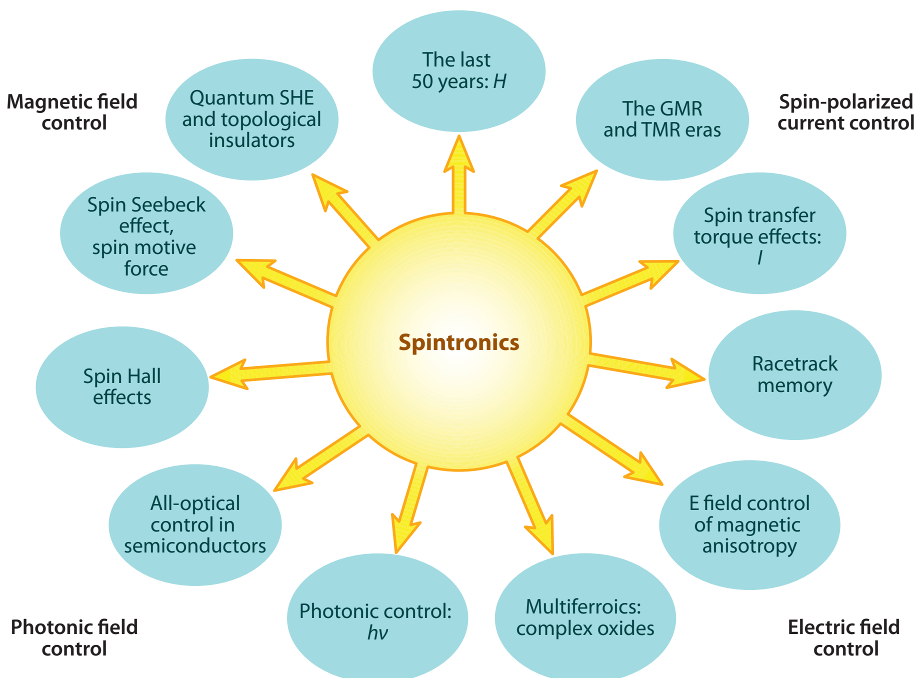

Figure 1

Overview of phenomena featured in this review.

uses protein or viral capsid scaffolds adds another layer of novelty to hierarchical assembly processes to create entire devices or complex subassemblies (16). This provides a retort to the criticism that self-assembly will never work because it is stochastic.

In a technical comparison with living mammals, the IBM Blue Gene/L® multiprocessor supercomputer showed a close match to the processing power of the brain of a mouse (17)! This is quite astounding, given the large mismatch in the volume, weight, and cooling capacity of the two. Thus, although silicon technology should be capable of pressing on to single-digit length scales, one should not dismiss the power of self-assembly on the basis of its stochastic limitations.

This introduction provides examples of the impact of spintronics intellectually and in the world of information technology, and its relationship to the emerging fields of nanoscience and ultrafast science. The brief discussion of measurement techniques and fabrication methods provides useful background references. In the following section, we focus on recent enabling phenomena that permit spintronic functionality to prevail in the absence of external magnetic fields. Thus, whereas the past 50-plus years represented the age of magnetic field control of the magnetization orientation, and hence of the binary coding of stored magnetic information (recent highlights include GMR devices and today's TMR devices), the future holds in store even newer phenomena. These include control via spin-polarized electric currents and via electric fields and photonic fields. **Figure 1** shows a sunburst schematic that encompasses each of the subsections of Section 2 on spintronic phenomena. Section 2 begins with a discussion of spin transfer torque (STT) effects and, moving clockwise around **Figure 1**, ends with a cursory discussion in Section 2.9 of the quantum spin Hall effect (QSHE) and topological insulators. We end with Section 3, which contains a brief summary and concluding remarks. We do not attempt to be all-inclusive in the referencing. The purpose of the review is to provide a glimpse of where action is needed to lead to new opportunities in the future, as seen through the eyes of the authors.

2. PHENOMENA

2.1. Spin Transfer Torque

A spin-polarized electric current can be used to switch the magnetization of a nanoscale memory element. This is an example of an STT effect. It can be envisioned as the inverse of a current becoming polarized by passing through a magnetized medium due to spin-dependent scattering processes. STT requires a large spin current passing through a small passageway. Hence, a preferred geometry is that of the nanopillar. Ralph & Stiles provide an outstanding recent overview of STT effects (18). STT was first theoretically uncovered and popularized by Slonczewski (19) and Berger (20). Thus, the first step to exploring STT effects is to produce spin-polarized currents. Whereas an ordinary electric current has equal populations of spin-up and -down electrons, a spin-polarized current necessarily has unequal populations. Different techniques are used to illustrate the generation of spin-polarized currents, for example, running a current through a magnetized medium, which results in spin-dependent scattering processes. (We explore the exotic case of pure spin currents in the absence of charge currents in Section 2.7.)

An exciting development is the exploration of STT effects in their many different experimental and theoretical manifestations (21–25), including nano-oscillators (26) and a novel method of switching MTJs, which enables a scaling of magnetic random access memory (MRAM) (27, 28). For the past 50 years, the only way to switch or excite magnetic moments was by using magnetic fields, but magnetic fields are extremely detrimental from a device perspective. The problem is that as devices shrink in size, larger and larger magnetic anisotropies are necessary to prevent them from being disturbed by thermal fluctuations as the superparamagnetic limit is approached, which means larger magnetic fields are also necessary to write and switch them. This then requires ever-bigger electrical currents pulsing through copper wires to create the Oersted fields, which are incompatible with the required smaller transistors of scaled-down complementary metal oxide semiconductor (CMOS) devices. This brings us back to the STXM example in Section 1, where the magnetization dynamics of vortices in permalloy nanostructures were imaged as they gyrated in response to high-frequency, spin-polarized electric currents passing through them (14). The point of the experiment was to evaluate what fraction of the dynamics to attribute to STT effects and what fraction to attribute to Oersted fields produced by the large magnitude of the spin-polarized currents used. The conclusion was that the dominant effects were STT effects, but the Oersted-field effects were non-negligible. Finally, it also has been suggested that a simple way to quantitatively study STT is by its effect in Doppler shifting spin waves or magnons (29). A recent conference entitled *Magnonics* provided its attendees with new information about using magnons to study STT.

2.2. Racetrack Memory

In the past few years, it has been recognized that domain walls can be manipulated by STT. From this, an entirely new type of spintronic device has emerged that has the potential to replace hard disk drives: the racetrack memory. The racetrack consists of a ferromagnetic nanowire that is encoded with magnetic domains. Spin-polarized current pulses coherently transport the domain walls along the wire past read and write devices. The wire is approximately twice the length of the stored information; therefore the motion of the domain walls can be bidirectional. A schematic of the racetrack is shown in **Figure 2** in vertical (**Figure 2*a***) and horizontal (**Figure 2*b***) configurations. The read function is shown (**Figure 2*c***) via TMR and the write function (**Figure 2*d***) via stray fields, and arrays for high-density storage are depicted (**Figure 2*e***). The beauty of the vertical racetrack concept is that it not only eliminates motors and disk crashes, but moves toward three-dimensional, nonvolatile architectures. Each track is serviced by one read and write device, making access time potentially highly competitive. Depending on the number of domain walls per track, the bit packing density and cost can become highly competitive. Thus, the racetrack, or a concept like it, could someday not only replace the hard disk but could also start to encroach on the realm of logic devices.

Although magnetic logic devices might not be available until the distant future, we know that today's leaky silicon transistor is a source of concern in terms of electrical power usage worldwide and of the concomitant greenhouse gas emissions due to much of today's electricity being derived from coal (31). Thus, spintronics research is being closely monitored to see whether it can offer alternatives that will be environmentally and economically attractive in the future. In this spirit, another recent effort to reduce power consumption and interconnect delay via three-dimensionally configuring MTJs is the interesting logic-in-memory architecture of Matsunaga et al. (32) who fabricated a nonvolatile full adder.

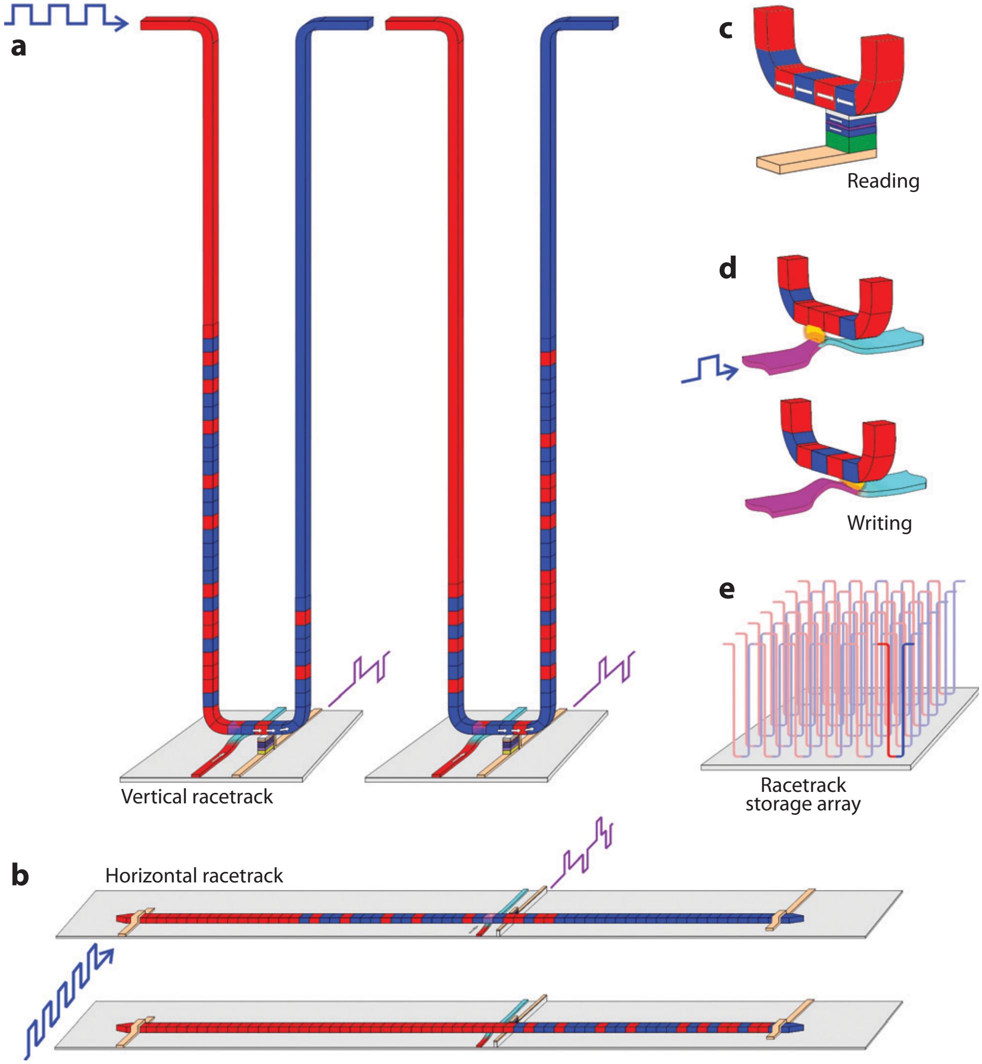

Figure 2

Schematics of racetrack memory. (*a*) A vertical configuration. The two drawings show magnetic track patterns before and after domain walls have moved past the read and write devices. (*b*) A horizontal configuration. (*c*) Data are read by measuring the tunneling magnetoresistance (TMR) of a magnetic tunnel junction (MTJ) connected to the racetrack. (*d*) Data can be written, for example, utilizing the fringing fields from a domain wall moved in a ferromagnetic nanowire oriented orthogonal to the storage nanowire. (*e*) Arrays of racetracks on a chip. Taken from Parkin et al. (30). Reprinted with permission from AAAS.

2.3. Electric Field Control of Magnetic Anisotropy

Other new means of manipulating magnetic moments and electron spins are electric fields and photon fields. There are two ways by which electric fields have recently been demonstrated to control magnetic properties: one is to manipulate the magnetic anisotropy of ultrathin Fe-based structures, and the other is in multiferroic systems that have coupled magnetic and ferroelectric order parameters. Weisheit et al. (33), in a proof-of-principle experiment, demonstrated electric field–induced modification of the coercivity of ultrathin FePt and FePd intermetallic electrodes in an electrochemical cell, as detected via the polar magneto-optical Kerr effect. They attributed the result to a change in the *d*-band filling with the application of the field. Subsequently, Ohta et al. (34) reported the voltage-controlled in-plane magnetic anisotropy of Fe/*n*-GaAs(001) Schottky junctions at room temperature using a perpendicular electric field. The maximum change observed was 4.5% of the saturation magneto-optic Kerr ellipticity signal, but the mechanism responsible for the change was unclear. However, members of this same team published a paper two days earlier using the same magneto-optic approach; Maruyama et al. (35) reported an ∼40% voltage-induced change in perpendicular magnetic anisotropy of an ultrathin Fe/MgO(001) junction and had numerous ideas to explain their results based on band structure filling effects, anisotropy energetics, and macrospin simulations. An important point made by both papers was the speculation that such functionality could lead to low-power magnetization switching, and hence, to low-power logic devices and nonvolatile, solid-state memory.

2.4. Multiferroics

Multiferroic systems that have coupled magnetic and ferroelectric order parameters are fascinating from a basic standpoint, and they are also useful because electric fields can potentially be used to switch the magnetization. Electric fields can be generated via voltages, which are local, as opposed to magnetic fields, which are nonlocal and can adversely influence neighboring bits. Why, then, are there so few magnetic ferroelectrics? Nicola Hill (36) (also known as Nicola Spaldin) asked this prophetic question in 2000. Hill concluded that magnets likely thrive on d electrons, whereas ferroelectrics at best only tolerate them under certain conditions. Rondinelli et al. (37) continue to pursue the answer in their recent paper. However, the research concluded that experimentalists should search for the answer. Early experimental and theoretical studies of magnetic ferroelectrics are reviewed by Smolenskii & Chupis (38), although seminal ideas can be traced back to Pierre Curie's 1894 paper (39). Kimura et al. (40) discovered magnetic control of the ferroelectric polarization in single crystalline perovskite $TbMnO_3$ for which the effect of spin frustration causes a sinusoidal antiferromagnetic (AF) ordering at low temperatures (∼41 K). The modulated magnetic structure is accompanied by lattice modulations that are magneto-elastically induced; thus frustrated spin systems seem to be candidates in the search. Wang et al. (41) explored perovskite $BiFeO_3$ epitaxial films grown via pulsed laser deposition onto $SrTiO_3$ substrates. Bulk $BiFeO_3$ is a well-studied multiferroic of rhombohedral crystal structure whose ferroelectric Curie temperature is ∼1103 K and AF Neél temperature is 643 K. The films were reported to be monoclinic and to have exceptional magnetic, ferroelectric, and coupled properties at room temperature, exceeding those of the bulk (41). Much work since has focused on $BiFeO_3$. In recent work, Seidel et al. (42) report on the electronic conductivity of ferroelectric domain walls of the three low Miller index faces of $BiFeO_3$ at room temperature. This work confirms the early report of the uniqueness of the properties of $BiFeO_3$ films relative to their bulk counterparts (41), and it emphasizes that their domain walls, measuring only ∼2 nm in width, can act as functional units for future applications.

2.5. Photonic Control

Another way to switch the magnetization is with ultrafast light pulses. Experiments by Stanciu et al. (43) have broken new ground in this emerging area. They have placed amorphous GdFeCo ferrimagnetic alloy film samples, prepared as multilayers with capping-, buffer-, and heat-sink layers, in a polarizing microscope and subjected them to 40-fs circularly polarized laser pulses ($\lambda = 800$ nm). The ultrafast light pulses act in two ways upon the system: (*a*) They rapidly heat the spin system to near the magnetic ordering temperature ($T_C = 500$ K), where switching becomes easy to achieve; and (*b*) via an inverse Faraday effect, in which the left and right circular lights in theory act as magnetic fields of opposite sign to cause the switching. Recently, members of this team followed the reversal process in real time via single-shot pump-probe microscopy in combination with atomic-scale simulations. Vahaplar et al. (44) showed that the reversal takes place via a strongly nonequilibrium state, called a linear reversal, and demonstrated a read-write time of 30 ps and estimated a 10-ps timescale for a 30-nm domain size.

Members of this team also studied the spin reorientation of the canted antiferromagnet $HoFeO_3$ in response to 100-fs circularly polarized light pulses in pump-probe experiments (45). They determined that reorientation occurs long after the initial stimulus is gone, as illustrated schematically in **Figure 3**. They refer to it as an inertia-driven spin-switching mechanism in antiferromagnets, whereby the system acquires sufficient momentum and energy to overcome the potential barrier and switch states after the stimulus has passed. They provided an enlightening discussion of the dynamics of field- and heat-driven reorientations and related their results to the ultimate speed of addressing a bit, as well as switching the bit, which might take much longer. An interesting aspect of these studies is

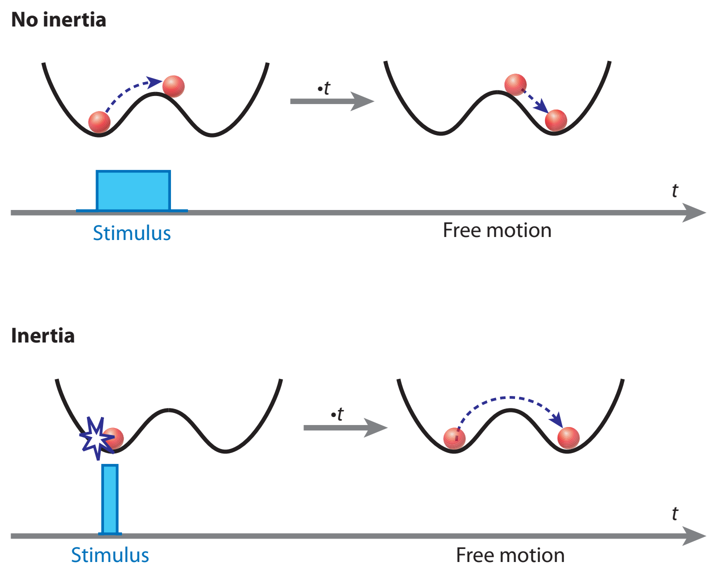

Figure 3

Schematic illustrating a striking new effect in ultrafast science identified as inertia-driven spin switching in antiferromagnets. The top panel shows the conventional, noninertial mechanism to switch between two potential wells for a canted antiferromagnet, where the circularly polarized laser pulse lasts long enough to drive the system over the potential barrier. The bottom panel illustrates the inertial mechanism whereby a fast pulse ends well before the transition is hardly initiated, but the system acquires sufficient momentum to subsequently overcome the barrier. Taken from Kimel et al. (45). Reprinted with permission from Macmillan Publishers Ltd. Copyright (2009).

that the laser pulse becomes an ultrafast magnetic field pulse. This relates to pioneering experiments carried out a decade earlier at the Stanford Linear Accelerator Center, where relativistic electron beam pulses were shot through Co/Pt multilayers (46) and Co films (47) to produce ultrafast magnetic field pulses as short as 2 ps and to observe the magnetization reversal patterns in the films afterward, via Kerr microscopy. The realm of ultrafast science is barely tapped and undoubtedly holds many surprises.

2.6. All-Optical Control in Semiconductors

Spintronics can be divided into two distinct subfields: semiconductor spintronics and metal spintronics. Most of the examples above emanate from the metal spintronics realm. Semiconductor spintronics has the potential advantage of being able to integrate seamlessly with today's semiconductor electronics. Semiconductor spintronics is often concerned with materials that become magnetic because they are doped with magnetic 3*d*-transition metal elements (9). Hence, they are dilute magnetic semiconductors. A potential disadvantage is that they can be miniaturized only to the extent of capturing a few dopants, rather than, for example, toward an atomic or molecular level. One of the intense challenges is to understand the microscopic nature of their magnetism in terms of their electronic structure, especially given the randomness of the doping. What are the interactions between the holes and local moments, and what is the evolution of possible metal-insulator transitions in these systems? Studies of the optical properties of these systems and their interplay with

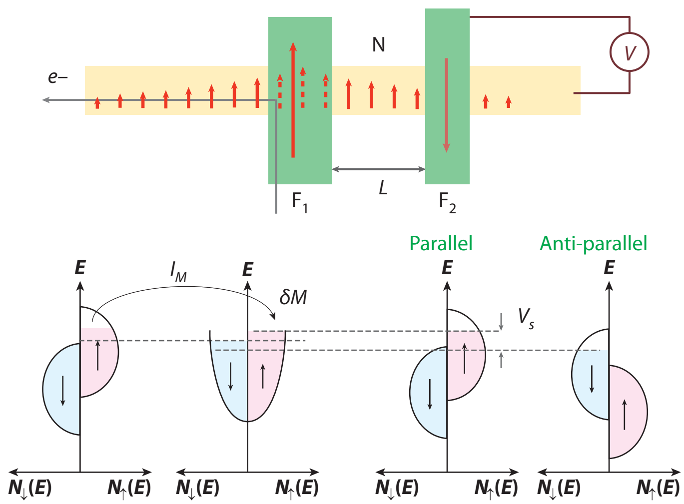

Figure 4

Concept of the lateral spin valve. F_1 and F_2 are two ferromagnetic electrodes (injector and detector, respectively) of different aspect ratios, so that they will switch their magnetization orientation in different magnitudes of an applied magnetic field. N is the nonferromagnetic metal that separates the two electrodes by a distance *L*. *N*(*E*) is the sub-band density of states for spin up or spin down, and the dashed horizontal lines on the *N*(*E*) plots are Fermi levels, in equilibrium at the left (assuming a half metallic ferromagnet, for simplicity) and out of equilibrium in the two plots to the right, due to the spin injection, where the mutual magnetization of F_1 and F_2 is parallel or antiparallel, as shown. V_s denotes a spin voltage. Taken from Bader et al. (64). Reprinted with permission from Elsevier. Copyright (2007).

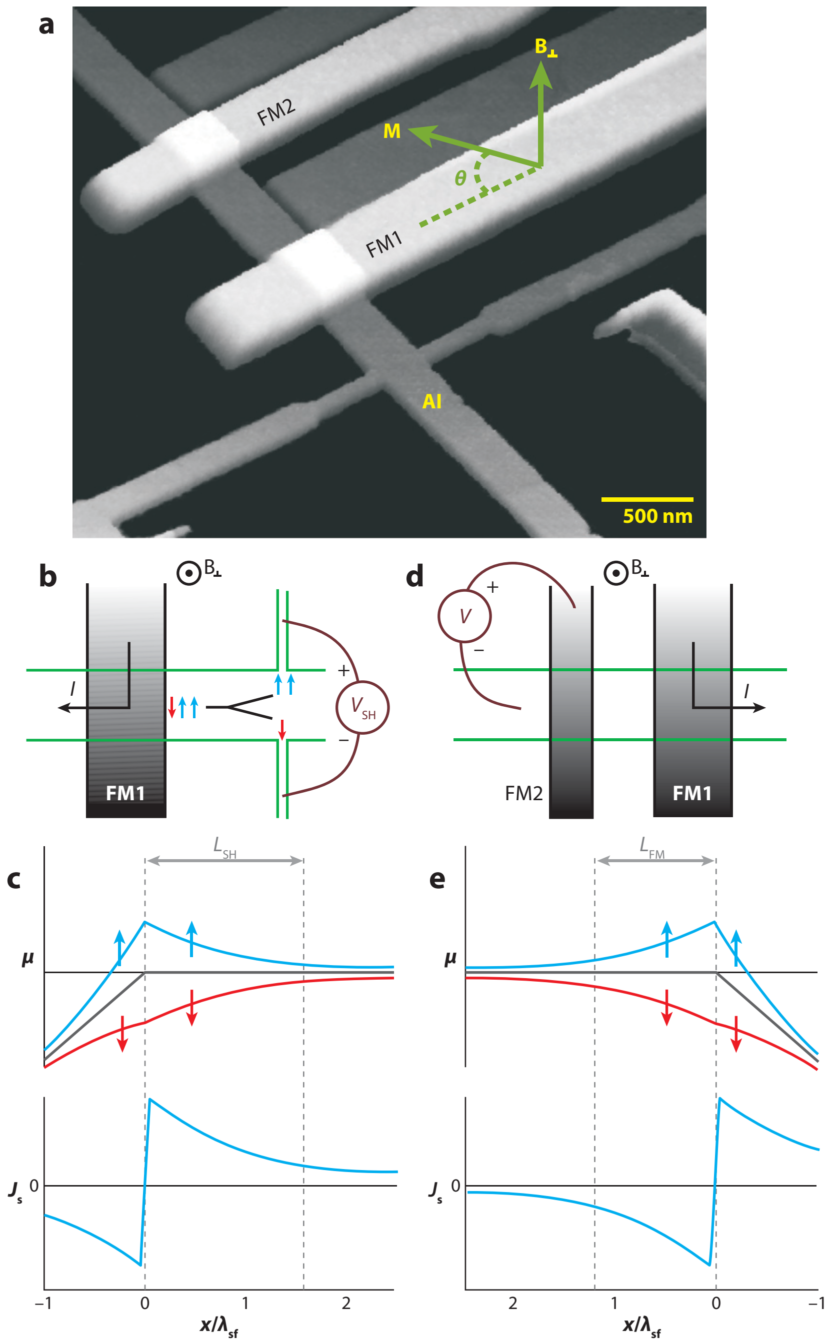
a
FM2
FM1
M
B⊥
θ
Al
500 nm
b
FM1
I
V_SH
+
−
B⊥
d
V
+
−
FM2
FM1
I
B⊥
c
L_SH
μ
J_s
0
−1
0
1
2
x/λ_sf
e
L_FM
μ
J_s
0
2
1
0
−1
x/λ_sf

theory are enormously useful in addressing these issues. A recent case study for the system of Mn doped into III-V semiconductor hosts provides a comprehensive view of the power of spectroscopic experiments to both provide basic insights and suggest future spin-optoelectronic devices (48).

In addition to providing global information about the system, optical techniques can function at the single-spin level. An impressive recent example is ^{15}N-doped diamond, where electron spin resonance spectroscopy at room temperature was used to study the spin structure of the orbitally excited state of its ^{15}N-vacancy centers. A large hyperfine splitting was reported relative to the ground state, but perhaps even more interestingly, dramatic strain sensitivity was observed that enables the individual centers to be spectroscopically differentiated from each other. Such studies could one day lead to ultrafast, all-optical quantum control of information. Another very important aspect of this system is that spin diffusion lengths tend to be limited by the spin-orbit interaction. The quest is for long spin diffusion lengths, which translates to low Z elements, such as carbon. For this reason, and because of its favorable thermal conductivity properties, diamond is an interesting host. As such, low Z also fuels the general interest in organic spintronics.

2.7. Spin Hall Effect and Inverse Spin Hall Effect

Historically, the progression here is twofold, with theory and experiment taking paths that were separated by decades in time. On the theory front, D'yakanov & Perel (49) made a brilliant prediction in 1971 about the existence of a spin Hall effect (SHE). SHE is the separation of spin-up and -down currents along opposite edges of a nanostructure (or meso-scale structure) induced by a transverse electric field due to the spin-orbit interaction. The prediction, however, necessarily languished in the literature until experimental capabilities were capable of the test. More recently, there has been a wealth of theoretical interest, as exemplified by the impurity scattering approach of Hirsch (50) and the diffusive scattering approach of Zhang (51), and as summarized by Kato et al. (52), who announced the first experimental detection of the SHE, as we mention below. On the experimental front, there was a learning curve involved in going from GMR multilayer films and the pioneering concept of the Johnson spin transistor (53–55) to its modern realization in terms of the metallic, nonlocal, lateral, spin valve, which was refined over the years by

Figure 5

An example of a spintronic device involving the detection of the spin Hall effect utilizing the lateral spin valve type geometry, as in **Figure 4**. (*a*) An atomic force microscope image of the device, which consists of a thin Al Hall cross that is oxidized and in contact with two ferromagnetic electrodes of different widths (FM1 and FM2). (*b*) The measurement where a current, *I*, is injected out of FM1 into the Al film and away from the Hall cross. A spin Hall voltage (V_{SH}) is measured between the two Hall probes. V_{SH} is caused by the separation of up and down spins due to the spin-orbit interaction in combination with a pure spin current. (*c*) The top panel shows the spatial dependence of the spin-up and -down electrochemical potentials μ, whereas the black line represents μ in the absence of spin injection. The bottom panel illustrates the associated spin current J_s. The polarized spins are injected near $x = 0$ and diffuse in both Al branches in opposite directions, decaying over a characteristic length scale. The sign change in J_s reflects the flow direction. (*d*) A spin-transistor measurement for device characterization, where *I* is injected out of FM1 into the Al film and away from FM2. An output voltage, *V*, is measured between FM2 and the left side of the Al film, where part *e* depicts the same quantities as in part *c*. The magnetic field is applied out of the plane of the device so the magnetization, *M*, is rotated by an angle, θ, as shown, because the easy axis is in plane. Taken from Valenzuela & Tinkham (62). Reprinted with permission from Macmillan Publishers Ltd. Copyright (2006).

groups in Europe (56–58), Japan (59), and the United States (60–63). **Figure 4** shows a schematic rendition of the concept of the lateral spin valve (64). This development was taken to the next level by Valenzuela & Tinkham (62) who utilized the laterally patterned configuration to provide an all-electrical detection of the SHE in a metallic system. Their experimental configuration and measurement trends appear in **Figure 5** (62; 65, see fig. 7.4 therein and related text). They used CoFe ferromagnetic electrodes and an Al crossbar separated by Al_2O_3 tunnel barriers. Remarkably, as mentioned above, two years earlier Kato et al. (52) were the first to detect the SHE effect in a semiconducting system. They did so by imaging the electrically induced opposite spin polarizations on opposite ends of channels on nonmagnetic semiconductors of unstrained GaAs and strained InGaAs in a Kerr microscope. There is still much discussion of the mechanisms associated with the SHE in magnetic and nonmagnetic systems, i.e., intrinsic (66) versus extrinsic (49, 50). This also raises the interesting topic of spintronics without magnetism, as recently addressed by Awschalom & Samarth (67). Seki et al. (68) provide another interesting report of a giant SHE in perpendicularly magnetized FePt/Au devices. Their device schematic is shown in **Figure 6**, and the unifying features can be seen in **Figures 4–6**. Reports of giant effects tend to be newsworthy because they hold the promise of providing strong signals to explore and potentially exploit. However, more recent work by Mihajlović et al. (69) on all-Au Hall bars (shown in **Figure 7**) describes an absence of a giant SHE. Thus, our understanding of the spin transport still requires further investigation.

The inverse SHE (ISHE) involves a spin current inducing a transverse charge current and causing a charge accumulation. The importance of the ISHE is that along with the SHE it provides the ability to reversibly convert charge and spin currents into one another. Thus, there is interest in both effects. The theoretical prediction of the ISHE came from Hankiewicz et al. (70). The first experimental realization in a semiconductor was reported in 1984 (71). In 2006, Saitoh et al. (72) reported the ISHE in spin-pumping ferromagnetic resonance experiments on the permalloy/Pt system. At resonance, the local spins transfer their angular momentum to the conduction electrons, causing the propagation of a pure spin current through the Pt, which leads to a transverse charge current and gives rise to a charge accumulation at the edges of the Pt that is detected as a potential difference. Also in

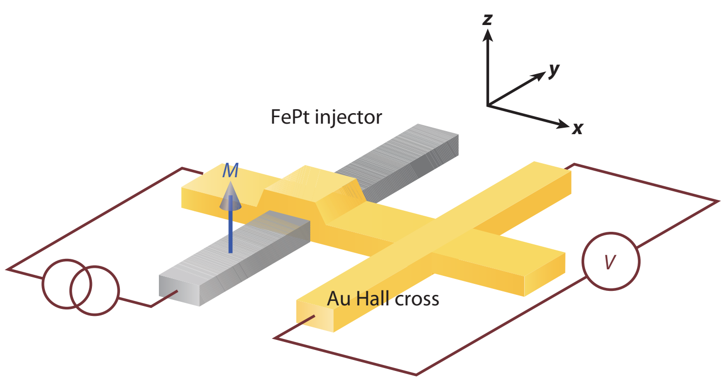

Figure 6

Measurement geometry in the experiment by Seki et al. (68) reporting giant spin Hall effect in perpendicularly spin-polarized FePt/Au devices. Reprinted with permission from Macmillan Publishers Ltd. Copyright (2008).

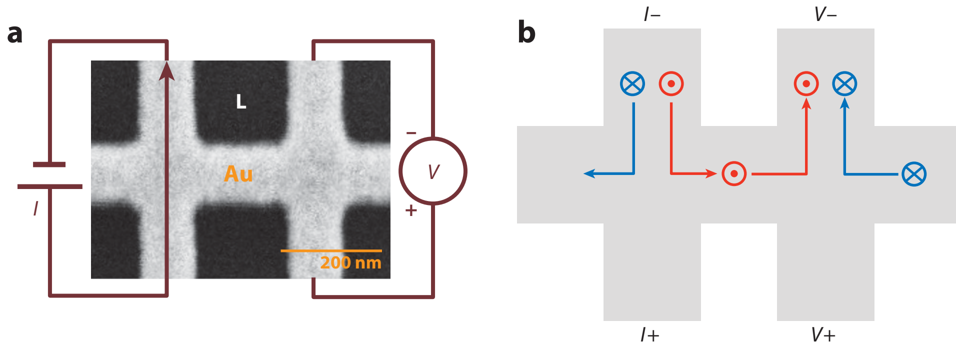

Figure 7

(*a*) SEM image and measurement geometry in field-free experiment reporting absence of giant spin Hall effect in mesoscopic Au Hall bars. (*b*) Schematic depicts the physical mechanism giving rise to the nonlocal spin Hall resistance, where red and blue colors represent spin-up and spin-down currents, respectively, and the spins are oriented perpendicular to the plane of the device. (The spin-down drift current from the right ensures charge neutrality.) Taken from Mihajlović et al. (69). Reprinted with permission from the American Physics Society. Copyright (2009).

2006, Valenzuela & Tinkham (62) reported the detection of the ISHE in a metallic system in the same study in which they detected the SHE. Kimura et al. (73) followed with another demonstration of the SHE and ISHE using a permalloy/Cu/Pt structure. The high Z of the Pt ensures a large spin-orbit interaction, and indeed Kimura et al. reported values of the spin Hall conductivity at room temperature in excess of 10^4 of that reported in semiconducting systems (73). Thus, the reciprocal SHE and ISHE appear in metals and semiconductors and are ripe for further study and to further stimulate the imagination.

2.8. Spin Seebeck Effect and Spin Motive Force

The spin Seebeck effect involves the generation of a spin voltage due to a temperature gradient across a metallic magnet. **Figure 8** shows a schematic comparison between a conventional thermocouple and the spin Seebeck effect. The first observation of the spin Seebeck effect resulted from advances in spin detection techniques involving the SHE and were reported by Uchida et al. (74). They used a permalloy sample of millimeter dimensions lined with Pt at the two far edges, across which the temperature gradient was applied; an in-plane magnetic field was applied across the gradient direction and cycled through hysteresis loops. The conventional Seebeck coefficient for spin-up and -down electrons differs, yielding a difference potential within each Pt electrode proportional to the temperature gradient, as shown in **Figures 8** and **9**. This difference potential provides a measure of the spin Seebeck effect. The beauty and power of this effect are that it can persist over macroscopic length scales, whereas all other effects involving the injection and propagation of pure spin currents tend to be limited by short spin diffusion lengths within the material. Thus, this research area appears to be quite promising.

Another impressive recent experiment where an electromotive force (emf) of spin-based origin was reported, along with magnetoresistance values as large as 10^5% in semiconductor-based MTJs, is the work of Hai et al. (75). The complex layering and processing of their junctions leave an active layer of zinc-blend-structure MnAs nanoparticles self-assembled within GaAs. Conduction across this maze is impeded by the

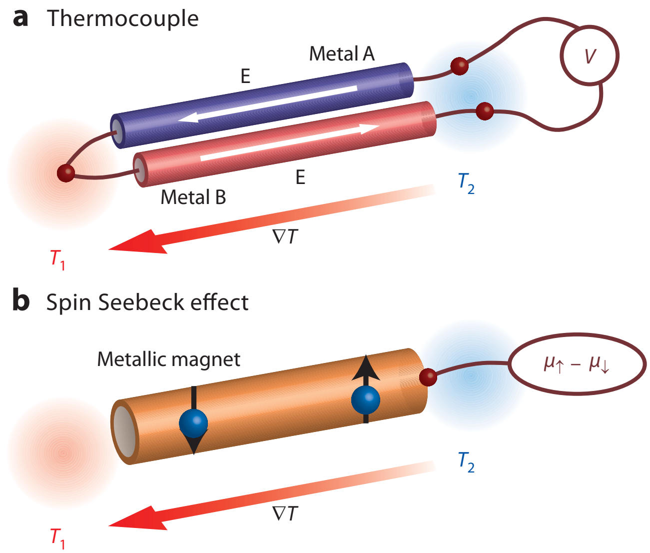

Figure 8

Illustration of a conventional thermocouple (*a*) and spin Seebeck effect (*b*). In part *b* the spin-up and -down bands have different Seebeck coefficients, leading to a spin voltage caused by the temperature gradient. The spin-dependent electrochemical potentials (μ) take on a spatial distribution along the temperature gradient so that one end is rich in down spins and the other is rich in up spins, as shown. Taken from Uchida et al. (74). Reprinted with permission from Macmillan Publishers Ltd. Copyright (2008).

Coulomb blockade effect. The spin structure is split by a magnetic field, but there is spin-flip mixing of channels at the 3 K temperature of the experiment. Under these conditions, there is a steady current driven by the emf associated with the relaxation within the ensemble of nanoparticles of two spin-state systems. The magnetoresistance is bias dependent and reaches its largest reported value at very small voltages (i.e., 1 mV). Hai et al. (75) suggest that the large magnetoresistance and the emf offer the possibility of new types of active devices, such as spin batteries. Additional recent examples of spin motive force studies include (*a*) a theoretical discussion of spin caloritronic effects in nanoscale magnetic structures by Hatami et al. (76), as well as (*b*) permalloy bridge experiments and a universal theory of the emf induced by domain wall motion by Yang et al. (77). The introduction in the latter paper presents a discussion of the topological aspects of the problem, which brings us to the next and last subsection of our review.

2.9. Quantum Spin Hall Effect and Topological Insulators

The quantum spin Hall state is time reversal invariant with a bulk band gap that supports edge states that are gapless to the transport of charge and spin. The QSHE and topological insulators are of interest because they give rise to dissipationless surface-edge currents. In the presence of spin-orbit coupling, certain topological insulators exhibit the QSHE in zero magnetic fields, supporting pure spin-polarized surface edge currents that are of fundamental interest. Because modern spintronics is very much invested in understanding the behavior of the physics of pure spin currents, the realm of spintronics and that of topological insulators

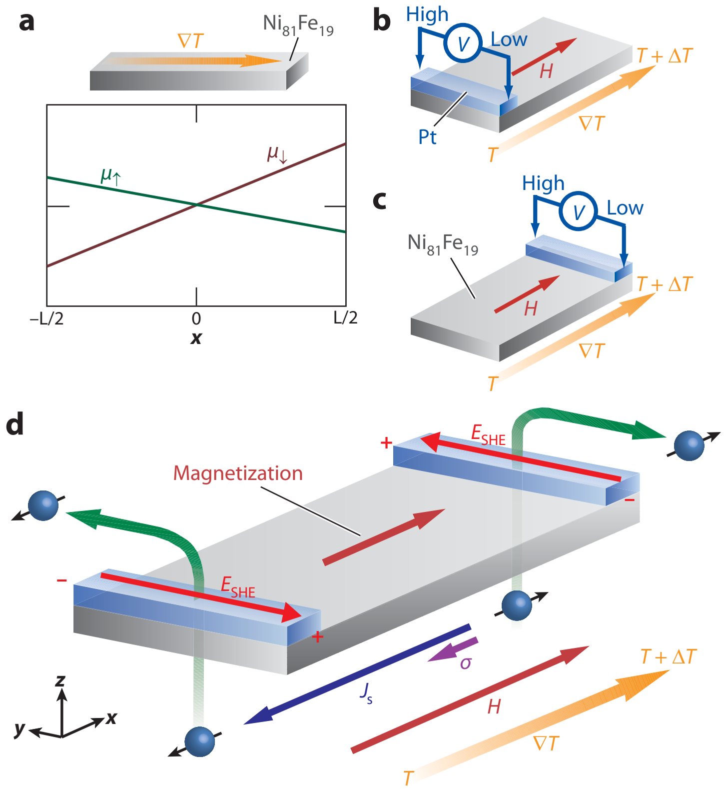

Figure 9

Measurement geometry in experiment reporting the spin Seebeck effect in a permalloy slab of dimensions 6×4 mm^2 lined on two opposite sides with Pt. Part *a* shows calculated electrochemical potentials, μ, across the temperature gradient for spin-up and -down electrons. Parts *b* and *c* are measurement setups. Part *d* illustrates the spin Seebeck effect induced in the permalloy by the temperature gradient, and the inverse spin Hall effect induced in the Pt wires attached to the film edges. J_s is the direction of the spin current in the film, and E_{SHE} is the emf generated by the ISHE in the wire. σ, the spin polarization vector of the spin current, lies along the magnetization axis. Taken from Uchida et al. (74). Reprinted with permission from Macmillan Publishers Ltd. Copyright (2008).

merge in a fertile manner. A fascinating recent prediction is that a charge placed above the surface of a topological insulator will be screened by these edge currents and will give rise to an image charge that looks like a magnetic monopole (78)! Kane & Mele (79) provide a group theoretical understanding of the topological order of the QSHE and use graphene as an illustration. They show that the quantum spin Hall state is unique from that of an ordinary insulator. Bernevig et al. (80) reported experiments on HgTe/CdTe semiconductor quantum wells in which they observed an electronic transition as a function of thickness. They identified their observation as a quantum phase transition between a conventional insulator and a topological insulator exhibiting a QSHE with a pair of helical edge states. König et al. (81) further confirmed that the HgTe quantum well system had the characteristics of a quantum spin Hall insulator at low temperatures. Hsieh et al. (82) recently examined bulk $Bi_{1-x}Sb_x$ single crystals for quantum Hall behavior utilizing angle-resolved photoelectron spectroscopy while modulating the incident photon energy. They searched for evidence of metallic surface states and confirmed that the $Bi_{1-x}Sb_x$ system provides yet another example of a topological insulator but has different symmetry than graphene. Graphene is such a rich and active field that it would require its own exclusive overview. From the point of view of spintronics, it possesses unique electronic properties, in addition to long spin lifetimes and long spin diffusion lengths. Tombros et al. (83) constructed nonlocal lateral spin valves utilizing cobalt electrodes in contact with single-layer graphene at room temperature via a thin oxide layer and reported spin relaxation lengths of 1.5–2 μm and spin polarization of the ferromagnetic contacts of 10%, which are quite respectable values. The future should provide further developments on the graphene front. The results discussed in this subsection, taken collectively, suggest that there is much basic research to be explored in understanding the topological diversity of quantum systems.

3. CONCLUSIONS

Spintronics can be divided into two distinct subfields: semiconductor spintronics and metal spintronics. The former has been rich in fundamental science but not as clear in its path to the world of applications. In the metal spintronics field, there has been a wealth of extremely important applications, the first of which is spin valve sensors for magnetic disk drives, which have been surpassed in the past few years by related devices based on the same spin-engineering concepts but utilizing spin-dependent tunneling. One of the most exciting developments in the past few years has been the demonstration of the switching of magnetic moments by spin-polarized currents, electric fields, and photonic fields. These phenomena will likely have important technological impact in the near future. Developments in the field of spintronics continue to be strongly dependent on the exploration and discovery of novel material systems. For example, one of the most exciting recent developments was the theoretical prediction and experimental verification of dissipationless spin-edge currents in a class of gapless semiconductors known as topological insulators. An array of novel transport and thermoelectric effects dependent on the interplay between spin and charge currents have been explored theoretically and experimentally in recent years. In summary, the field of spintronics continues to expand into new realms, with a rich and synergistic interplay between theory, experiment, and applications. Spintronics promises to have significant impact in the worlds of science and technology.

DISCLOSURE STATEMENT

The authors are not aware of any affiliations, memberships, funding, or financial holdings that might be perceived as affecting the objectivity of this review.

ACKNOWLEDGMENTS

S.D.B. is supported by the U.S. Department of Energy, Office of Science, Basic Energy Sciences, under contract no. DE-AC02-06CH11357.

LITERATURE CITED

1. Bader SD. 2006. *Rev. Mod. Phys.* 78:1–15 and references therein
2. Moodera JS, Kinder LR, Wong TM, Meservey R. 1995. *Phys. Rev. Lett.* 74:327376

3. Miyazaki T, Tezuka N. 1995. *J. Magn. Magn. Mater.* 139:231
4. Butler WH, Zhang X-G, Schulthess TC, MacLaren JM. 2001. *Phys. Rev. B* 63:054416
5. Mathon J, Umerski A. 2001. *Phys. Rev. B* 63:R220403
6. Ikeda S, Hayakawa J, Ashizawa Y, Lee YM, Miura K, et al. 2008. *Appl. Phys. Lett.* 93:082508
7. Jiang L, Naganuma H, Oogane M, Ando Y. 2009. *Appl. Phys. Express* 2:083002–5
8. Stöhr J, Siegmann HC. 2006. *Magnetism: From Fundamentals to Nanoscale Dynamics. Springer Ser. Solid-State Phys.*, Vol. 152. Berlin: Springer
9. Zhu Y, ed. 2005. *Modern Techniques for Characterizing Magnetic Materials*. New York: Kluwer Acad.
10. Zutic I, Fabian J, Sarma SD. 2004. *Rev. Mod. Phys.* 76:323–410
11. Freeman MR, Choi BC. 2001. *Science* 294:1484–88
12. Fitzsimmons MR, Bader SD, Borchers JA, Felcher GP, Furdyna JK, et al. 2004. *J. Magn. Magn. Mater.* 271:103–46
13. Srajer G, Lewis LH, Bader SD, Epstein AJ, Fadley CS, et al. 2006. *J. Magn. Magn. Mater.* 307:1–31
14. Kortright JB, Awschalom DD. 1999. *J. Magn. Magn. Mater.* 207:7–44
15. Bolte M, Meier G, Krüger B, Drews A, Eiselt R, et al. 2008. *Phys. Rev. Lett.* 100:176601
16. Liu C, Chung S-H, Jin Q, Sutton A, Yan F, et al. 2006. *J. Magn. Magn. Mater.* 302:47–51 and references therein
17. Parkin SSP. 2009. *The spin on electronics*. Presented at ICM-2009, July 27, Karlsruhe, Ger.
18. Ralph DC, Stiles MD. 2008. *J. Magn. Magn. Mater.* 320:1190–216
19. Slonczewski JC. 1996. *J. Magn. Magn. Mater.* 159:L1
20. Berger L. 1996. *Phys. Rev. B* 54:9353–58
21. Berkov DV, Miltat J. 2008. *J. Magn. Magn. Mater.* 320:1238–59
22. Beach GSD, Tsoi M, Erskine JL. 2008. *J. Magn. Magn. Mater.* 320:1272–81
23. Tserkovnyak Y, Brataas A, Bauer GEW. 2008. *J. Magn. Magn. Mater.* 320:1282–92
24. Ohno H, Dietl T. 2008. *J. Magn. Magn. Mater.* 320:1293–99
25. Haney PM, Duine RA, Núñez AS, MacDonald AH. 2008. *J. Magn. Magn. Mater.* 320:1300–11
26. Silva TJ, Rippard WH. 2008. *J. Magn. Magn. Mater.* 320:1260–71
27. Katine JA, Fullerton EE. 2008. *J. Magn. Magn. Mater.* 320:1217–26
28. Sun JZ, Ralph DC. 2008. *J. Magn. Magn. Mater.* 320:1227–37
29. Vlaminck V, Bailleul M. 2008. *Science* 322:410–13
30. Parkin SSP, Hayashi M, Thomas L. 2008. *Science* 320:190–94
31. *Gadgets and Gigawatts: Policies for Efficient Electronics*. 2009. Copenhagen: Int. Energy Agency (IEA). 424 pp.
32. Matsunaga S, Hayakawa J, Ikeda S, Miura K, Hasegawa H, et al. 2008. *Appl. Phys. Express* 1:091301
33. Weisheit M, Fähler S, Marty A, Souche Y, Poinsignon C, Givord D. 2007. *Science* 315:349–51
34. Ohta K, Maruyama T, Nozaki T, Shiraishi M, Shinjo T, et al. 2009. *Appl. Phys. Lett.* 94:032501
35. Maruyama T, Shiota Y, Nozaki T, Ohta K, Toda N, et al. 2009. *Nat. Nanotechnol.* 4:158–61
36. Hill NA. 2000. *J. Phys. Chem. B* 104:6694–709
37. Rondinelli JM, Eidelson AS, Spaldin NA. 2009. *Phys. Rev. B* 79:205119
38. Smolenskii GA, Chupis IE. 1982. *Sov. Phys. Usp.* 26:475–93
39. Curie P. 1894. *J. Phys.* (Ser. III) 3:393–415
40. Kimura T, Goto T, Shintani H, Ishizaka K, Arima T, Tokura Y. 2003. *Nature* 426:55–58
41. Wang J, Neaton JB, Zheng H, Nagarajan V, Ogale SB, et al. 2003. *Science* 299:1719–22
42. Seidel J, Martin LW, He Q, Zhan Q, Chu Y-H, et al. 2009. *Nat. Mater.* 8:229–34
43. Stanciu CD, Hansteen F, Kimel AV, Kirilyuk A, Tsukamoto A, et al. 2007. *Phys. Rev. Lett.* 99:047601
44. Vahaplar K, Kalashnikova AM, Kimel AV, Hinzke D, Nowak U, et al. 2009. *Phys. Rev. Lett.* 103:117201

45. Kimel AV, Ivanov BA, Pisarev RV, Usachev PA, Kirilyuk A, Rasing T. 2009. *Nat. Phys.* 5:727–31
46. Back CH, Weller D, Heidmann J, Mauri D, Guarisco D, et al. 1998. *Phys. Rev. Lett.* 81:3251–54
47. Back CH, Allenspach R, Weber W, Parkin SSP, Weller D, et al. 1999. *Science* 285:864–67
48. Burch KS, Awschalom DD, Basov DN. 2008. *J. Magn. Magn. Mater.* 320:3207–28
49. D'yakonov MI, Perel VI. 1971. *Phys. Lett.* 35:459–60
50. Hirsch JE. 1999. *Phys. Rev. Lett.* 83:1834–37
51. Zhang S. 2000. *Phys. Rev. Lett.* 85:393–96
52. Kato YK, Myers RC, Gossard AC, Awschalom DD. 2004. *Science* 306:1910–13
53. Johnson M, Silsbee RH. 1985. *Phys. Rev. Lett.* 55:1790–93
54. Johnson M. 1993. *Phys. Rev. Lett.* 70:2142–45
55. Johnson M. 1993. *Science* 260:320–23
56. Jedema FJ, Filip AT, van Wees BJ. 2001. *Nature* 410:345–48
57. Jedema FJ, Nijboer MS, Filip AT, van Wees BJ. 2003. *Phys. Rev. B* 67:085319
58. Jedema FJ, Heersche HB, Filip AT, Baselmans JJA, van Wees BJ. 2002. *Nature* 416:713–16
59. Kimura T, Hamrle J, Otani Y, Tsukagoshi K, Aoyagi Y. 2004. *Appl. Phys. Lett.* 85:3501
60. Valenzuela SO, Tinkham M. 2004. *Appl. Phys. Lett.* 85:5914–16
61. Ji Y, Hoffmann A, Jiang JS, Bader SD. 2004. *Appl. Phys. Lett.* 85:6218
62. Valenzuela SO, Tinkham M. 2006. *Nature* 442:176–79
63. Garzon S, Zutić I, Webb RA. 2005. *Phys. Rev. Lett.* 94:176601
64. Bader SD, Buchanan KS, Chung S-H, Guslienko KY, Hoffmann A, et al. 2007. *Superlattices Microstruct.* 41:72–80
65. Comm. CMMP 2010. Natl. Res. Counc. 2010. Solid State Sci. Comm. 2007. *Condensed-Matter and Materials Physics: The Science of the World Around Us*. Washington, DC: Natl. Acad. Press, p. 133
66. Sinova J, Culcer D, Niu Q, Sinitsyn NA, Jungwirth T, MacDonald AH. 2004. *Phys. Rev. Lett.* 92:126603
67. Awschalom D, Samarth N. 2009. *Physics* 2:50
68. Seki T, Hasegawa Y, Mitani S, Takahashi S, Imamura H, et al. 2008. *Nat. Mater.* 7:125
69. Mihajlović G, Pearson JE, Garcia MA, Bader SD, Hoffmann A. 2009. *Phys. Rev. Lett.* 103:166601
70. Hankiewicz EM, Li J, Jungwirth T, Niu Q, Shen S-Q, Sinova J. 2005. *Phys. Rev. B* 72:155305
71. Bakun AA, Zakharchenya BP, Rogachev AA, Tkachuk MN, Fleisher VG. 1984. *JETP Lett.* 40:1293–95
72. Saitoh E, Ueda M, Miyajima H, Tatara G. 2006. *Appl. Phys. Lett.* 88:182509
73. Kimura T, Otani Y, Sato T, Takahashi S, Maekawa S. 2007. *Phys. Rev. Lett.* 98:156601
74. Uchida K, Takahashi S, Harii K, Ieda J, Koshibae W, et al. 2008. *Nature* 455:778–81
75. Hai PN, Ohya S, Tanaka M, Barnes SE, Maekawa S. 2009. *Nature* 458:489–92
76. Hatami M, Bauer GEW, Zhang Q, Kelly PJ. 2007. *Phys. Rev. Lett.* 99:066603
77. Yang SA, Geoffrey SD. 2009. *Phys. Rev. Lett.* 102:067201
78. Qi X-L, Li R, Zang J, Zhang S-C. 2009. *Science* 323:1184–87
79. Kane CL, Mele EJ. 2005. *Phys. Rev. Lett.* 95:146802
80. Bernevig BA, Hughes TL, Zhang S-C. 2006. *Science* 314:1757–61
81. König M, Wiedmann S, Brüne C, Roth A, Buhmann H, et al. 2007. *Science* 318:766–70
82. Hsieh D, Qian D, Wray L, Xia Y, Hor YS, et al. 2008. *Nature* 452:970–75
83. Tombros N, Jozsa C, Popinciuc M, Jonkman HT, van Wees BJ. 2007. *Nature* 448:571–75

Annual Review of Condensed Matter Physics

Volume 1, 2010

Contents

Errata

An online log of corrections to *Annual Review of Condensed Matter Physics* articles may be found at http://conmatphys.annualreviews.org/errata.shtml